Pathways for the Reaction of the Butadiene Radical Cation, $[C_4H_6]^{\bullet+}$, with Ethylene

Matthias Hofmann and Henry F. Schaefer, III*

Center for Computational Quantum Chemistry, University of Georgia, 1004 Cedar Street, Athens, Georgia, 30602-2525

Received: August 3, 1999

Reaction pathways for the addition of ethylene, **1**, to butadiene radical cation, **2**, involving H-shifts have been investigated at the coupled cluster UCCSD(T)/DZP//UMP2(fc)/DZP + ZPE level of theory. Activation energies are relatively low for [1,2]- (10.0 kcal mol^{-1}, **TS-4/20**) and [1,5]-hydrogen shifts (7.7 kcal mol^{-1}, **TS-4/26**) but are relatively high for [1,4]- (33.8 kcal mol^{-1}, **TS-4/14**) and [1,3]-H shifts (e.g. 42.2 kcal mol^{-1}, **TS-12/13**; 57.2 kcal mol^{-1}, **TS-16/21**). Several rearrangement reactions have been found to occur below the energy limit of separated **1** + **2**. The cyclopentenyl cation, $[C_5H_7]^+$, **18**, experimentally observed as reaction product of the butadiene radical cation, **2**, and ethylene, **1**, in the gas phase may origin from various reaction pathways. The following reaction sequence has been identified as the lowest in energy path from **1** + **2** to **18** with all relative energies ($\Delta E°$) of transition structures below that of **1** + **2**: (a) ethylene adds to the butadiene radical cation to form an open-chain distonic intermediate, **4**, that undergoes a [1,5]-H shift to the 1,4-hexadiene radical cation, **26**; (b) intramolecular [2+1] cycloaddition to methyl-cyclopenta-1,3-diyl intermediates, **22** and **24**, which can interconvert through a bicyclo[2.1.0]pentane radical cation, **23**; (c) [1,2]-H shift of **24** to the 3-methyl cyclopentene radical cation, **16**; (d) methyl radical loss to give cyclopenten-3-yl cation, **18**. Along this reaction pathway, ΔH^{298} changes by −18.1 kcal mol^{-1} (ΔG^{298} by −16.0 kcal mol^{-1}) and only transition structures low in energy (ΔH^{298} is below that of **1** + **2**; max. $\Delta G^{298‡} = 10.4$ kcal mol^{-1} for [1,5]-H shift relative to **1** + **2**) are involved. Ethylene, **1**, can also add to **2**, simultaneously accepting a transferred hydrogen to give a 1,3-hexadiene radical cation. Back dissociation of the latter into **1** + **2** is favored over methyl radical loss.

Introduction

The Diels−Alder (DA) reaction,[1] a [4+2] cycloaddition used to build six membered rings, is one of the most valuable cycloadditions in organic chemistry. In cases where the ene does not add to the diene (even with the help of Lewis acids which may reduce the electron density of one reactant by complexation) one electron oxidation (by an oxidizing agent or by photoinduced electron transfer (PET)[2]) may accelerate the reaction. This approach has been termed "hole catalysis" by Bauld.[3] The radical cation reactions, which do not need to be electrocyclic reactions as well, generally have low activation energies but nevertheless show high degrees of peri-, regio-, and stereoselectivity.[4] The radical cation reactions thus complement the neutral reactions, and there are a number of applications of synthetic interest.[4−9]

Closed shell pericyclic reactions are quite well understood through the Woodward−Hoffmann rules[10] and the frontier orbital concept.[11] But even qualitative concepts are lacking for the radical cation reactions. Therefore, more detailed insights into the mechanisms of these reactions are desirable. Experiments deal with highly substituted molecules, in most cases. Computations, however, are ideal to study the parent reactions and to reveal important intrinsic features.

The only experimental investigation of the parent reaction of ethylene with the butadiene radical cation are recent experiments under low-pressure conditions conducted in a Fourier transform ion cyclotron resonance spectrometer with an external ion source.[12] By using deuterated reactants, Bouchoux and Salpin concluded that the intermediate $[C_6H_{10}]^{\bullet+}$ collision complex may evolve via two competitive channels: (a) methyl radical loss leading to the cyclopentenyl cation $[C_5H_7]^+$ preceded by extensive exchange of all hydrogen atoms and (b) ethylene loss (with one methylene group from the neutral reactant and one methylene group from the terminal position of the butadiene radical cation) leading to the butadiene radical cation. Under the low-pressure conditions in effect no efficient deactivation is possible and, hence, no $[C_6H_{10}]^{\bullet+}$ adduct could be detected.

Derrick, Fallick, and Burlingame investigated the reverse reaction, the dissociation of ionized cyclohexene into butadiene radical cation and ethylene, by field ionization mass spectrometry.[13] By using 3,3,6,6-tetra deuterated cyclohexene they found that this formally retro Diels−Alder reaction is preceded by hydrogen scrambling which was proposed to be a result of successive 1,3-allylic rearrangements. In addition to the butadiene radical cation (=$[M-C_2H_4]^{\bullet+}$), $[C_5H_7]^+$ (=$[M-[CH_3]^{\bullet}]^+$) and $[C_3H_5]^+$ (=$[M-[C_3H_5]^{\bullet}]^+$) were also dedected.

We recently investigated the reaction pathways connecting ethylene, **1**, and both *cis*- (**2**) and *trans*-butadiene radical cation (**9**) to the cyclohexene radical cation, **6**.[14] A stepwise addition involving an ion−molecule complex **3** and two open chain distonic radical cation conformers, **4** and **5**, (path **A**, Scheme 1) was predicted to have a low activation barrier of $\Delta G^{298‡} = 6.3$ kcal mol^{-1}. All intermediates and transition states for this path are lower in energy on the $E°$ potential energy surface. Haberl et al. showed that **4** can directly ring close to **6** without the involvement of intermediate **5**.[15] Another stepwise addition (path **B**) with one intermediate **7** could only be geometry optimized at the SCF (UHF/6-31G*) but not at correlated levels (UMP2 and UB3LYP/DZP). Higher level single-point calcula-

10.1021/jp9927707 CCC: $18.00 © 1999 American Chemical Society
Published on Web 10/21/1999

SCHEME 1

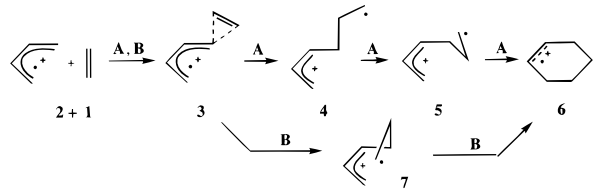

SCHEME 2

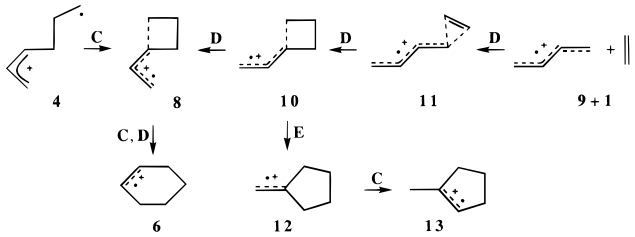

tions on the SCF stationary point, however, suggested that this path **B** in reality might be a highly nonsynchronous concerted addition with no or a very small activation energy. A cyclobutanation/vinylcyclobutane−cyclohexene rearrangement path **C** (Scheme 2) is competitive with path A because the barrier for the radical cation is drastically reduced ($\Delta G^{298\ddagger} = 8.0$ kcal mol^{-1}) compared to the neutral reaction[16] (48.6 kcal mol^{-1}). This route also allows *trans*-butadiene radical cation, **9**, to add ethylene, **1**, (via path **D**) as easily as the *cis* isomer (without prior cis/trans isomerization, which requires a relatively large 24.9 kcal mol^{-1} activation[17]) because the endo-/exo-isomerization of the intermediate vinylcyclobutane radical cation (**10** to **8**) has a transition state lower in energy than the critical ring expansion step from **8** to **6**. One path not ending in a six membered ring was already considered in ref 14 namely the ring expansion of *exo*-vinylcyclobutene radical cation **10** without prior isomerization to the endo form. This path **E** involves also a hydrogen shift and leads to the methylenecyclopentane radical cation **12** with an effective barrier ($\Delta E^{\ddagger}$) only 1.3 kcal mol^{-1} larger than path **D**. In this paper we extend our earlier study, which focused on the formation of the cyclohexene radical cation from the butadiene radical cation, $[C_4H_6]^{\bullet+}$, plus ethylene, C_2H_4, to reactions of the butadiene radical cation/ethylene system to include hydrogen shift reactions and thus explain the experimental observations on $[C_6H_{10}]^{\bullet+}$ in the gas phase. Under these low-pressure conditions the addition product cannot be deactivated and hence, no cyclohexene radical cation formation can be expected to be detected.

Computational Details

The same procedure as in ref 14 was applied here. The Gaussian 94 program[18] was used throughout this work. All structures were fully optimized consecutively at the UHF/3-21G, UHF/6-31G*, UMP2/6-31G*, UMP2/DZP, and B3LYP/DZP levels of theory. MP2 calculations made use of the "frozen core" approximation, i.e., only valence electrons were considered in the electron correlation treatment. Basis sets used are Pople's 3-21G and 6-31G* and the double ζ quality basis set of Huzinaga[19a] ("DZP") in the contraction scheme recommended by Dunning[19b] ((9s5p) contracted to [6111,41] for C and (4s) contracted to [31] for H). The exponent of the polarization functions (d type for C and p type for H) in DZP was 0.75.[20] Density functional theory (DFT) calculations employed Becke's three parameter exchange functional[21] and the correlation functional of Lee, Yang, and Parr, which includes both local and nonlocal terms,[22] as implemented in Gaussian 94.[18,23] But not all stationary points could be localized with B3LYP/DZP because currently used functionals (including the popular B3LYP) run into problems when combination or separation of spin and charge in radical ions is to be described. This was recently pointed out and discussed by Bally and Sastry.[24]

Therefore, UMP2(fc)/DZP geometries are discussed in the text unless stated otherwise. Vibrational frequencies have been computed at all levels of optimization for clarification of the nature of the stationary points and for zero-point vibrational energies (ZPEs). Relative energies are ZPE corrected applying scaling factors of 0.89, 0.93, and 1.0 for UHF, UMP2, and UB3LYP, respectively. Single energy points have been computed for UMP2(fc)/DZP geometries at the coupled cluster level including single and double excitations with perturbative estimation of triple corrections and using the DZP basis set and a UHF reference wave function (UCCSD(T)/DZP).[25] Thermal corrections for $T = 298.15$ K to enthalpies (ΔH^{298}) and free Gibbs energy values (ΔG^{298}) have been derived from unscaled frequencies. Unless specified otherwise, relative energies ($\Delta E°$) reported in the text are obtained at the coupled cluster level (UCCSD(T)/DZP//UMP2(fc)/DZP + 0.93 ZPE(UMP2(fc)/ DZP)) for $T = 0$ K. These values have also been used in the sketches of the reaction paths **F**−**I**. Whenever ΔG^{298} energies are discussed (because entropy effects are important) this is explicitly stated. Energy values in Table 1 and in Charts 1−4 are given relative to the cyclohexene radical cation which was chosen as a reference because of its very small spin contamination ($S^2 = 0.756$ at UHF/DZP//UMP2(fc)/DZP, ideal 0.750 for a doublet). Some structures (mostly transition structures) have S^2 expectation values significantly larger than 0.75. However, we are convinced that this is not problematic for our MP2 geometry optimizations because $\langle S^2 \rangle$ is still much closer to the doublet (0.75) than to the quartet value (3.75) even in the worst case (0.96). "Spin-projected energies" (PMP2 in Table 1) and coupled cluster energies are not deteriorated much by spin contaminated reference wave functions, in any case. Table 2 lists charges obtained from natural population analyses (NPAs);[26] hydrogen charges were summed into carbon atoms they are attached to.

Results and Discussion

Bouchoux and Salpin[12] were able to identify two different reactions between a butadiene radical cation and ethylene in their gas phase experiments: (1) methylene group transfer between (partially deuterated) butadiene radical cation and ethylene and (2) methyl radical loss of the $[C_6H_{10}]^{\bullet+}$ intermediate to give $[C_5H_7]^+$. Considering the heats of formation (and the thermal energies) of the compounds involved in the reaction 1,

$$\text{butadiene radical cation} + \text{ethylene} \rightarrow \text{methyl radical} + [C_5H_7]^+ \quad (1)$$

the authors concluded that the $[C_5H_7]^+$ species is a cyclopentenyl cation or a pentadienyl cation. The observed proton affinity pointed to the former. Inspired from these findings, we have looked into alternative pathways not leading to the radical cation of cyclohexene but to the cyclopentenyl cation and the methyl radical. For the formation of a methyl group, these pathways have to include hydrogen shifts at some point.

We have previously considered the ring expansion reaction of the *exo*-vinylcyclobutane radical cation, **10**, which involves

TABLE 1: Relative Energies[a] in kcal mol^{-1} for $[C_6H_{10}]^{\bullet+}$ Stationary Points

	6	**1 + 2**	**3**	**TS-3/4**	**4**
UMP2[b]	0.0	52.2	44.8	48.1	38.4
(S^2)	(0.756)	(0.926)	(0.919)	(1.076)	(0.763)
PMP2[b]	0.0	47.4	39.4	37.4	37.7
CCSD[d]	0.0	45.8	41.3	41.3	38.3
CCSD(T)[b]	0.0	45.6	39.0	38.9	36.9
ΔH^{298} [c]	0.0	47.1	40.2	39.8	38.1
ΔG^{298} [c]	0.0	33.5	35.8	36.2	34.1
//B3LYP/DZP	0.0	42.3	32.3	32.6	32.3

	TS-4/14	**14**	**TS14/15**	**15**	**TS15/16i**	**TS15/16r**	**16**	**TS-16/17**
UMP2[b]	68.6	9.4	28.4	14.9	38.7[d]	47.3	2.5	25.6
(S^2)	(0.767)	(0.780)	(0.756)	(0.781)	(0.826)	(0.891)	(0.756)	(0.812)
PMP2[b]	67.7	8.3	28.5	13.8	36.5[d]	42.4	2.5	23.8
CCSD[b]	74.3	12.5	28.8	17.9	37.4[d]	47.6	3.0	26.0
CCSD(T)[b]	70.7	11.1	28.4	16.3	35.4[d]	45.1	2.4	24.5
ΔH^{298} [c]	71.5	11.9	28.7	16.9	36.9[d]	45.2	2.6	25.3
ΔG^{298} [c]	68.8	9.1	27.0	14.8	33.8[d]	44.2	1.6	22.0
//B3LYP/DZP	59.7	8.8	25.1	14.5	33.3	43.7	1.8	*e*

	17	**18 + 19**	**TS-4/20**	**20**	**TS-20/21**	**21**	**TS-16/20**	**TS-16/21**
UMP2[b]	25.1	27.7	58.6	14.9	41.6	2.5	48.4	57.8
(S^2)	(0.779)	(0.761)	(0.956)	(0.841)	(0.955)	(0.756)	(0.963)	(0.761)
PMP2[b]	24.1	27.1	50.4	11.6	33.4	2.5	43.3	57.4
CCSD[b]	26.1	28.8	49.8	17.1	34.8	2.9	43.2	60.9
CCSD(T)[b]	24.8	27.7	46.9	15.4	34.0	2.4	40.5	59.6
ΔH^{298} [c]	26.3	29.0	47.5	16.0	34.4	2.6	40.9	59.4
ΔG^{298} [c]	20.6	17.5	44.7	14.3	32.4	1.7	39.0	59.2
//B3LYP/DZP	*f*	27.8	41.2	13.0	28.6	2.5	38.7	65.3

	TS-21/22	**22**	**TS-16/22**	**TS-22/23**	**23**	**TS23/24**	**24**	**TS16/24**
UMP2[b]	24.1	21.4	49.5	31.9	20.9	33.6	25.4	26.2
(S^2)	(0.765)	(0.764)	(0.766)	(0.767)	(0.783)	(0.767)	(0.764)	(0.763)
PMP2[b]	23.5	20.7	48.6	31.0	19.2	32.7	24.7	25.5
CCSD[b]	25.3	25.5	52.6	29.5	22.4	30.7	27.1	26.1
CCSD(T)[b]	24.3	24.3	51.2	28.3	21.1	29.5	26.6	25.6
ΔH^{298} [c]	24.3	24.6	51.1	28.4	21.3	29.5	26.8	25.6
ΔG^{298} [c]	23.6	23.5	50.6	27.2	20.5	28.7	25.7	24.8
//B3LYP/DZP	23.9	23.8	52.6	27.5	24.9	*g*	23.6	*h*

	TS-23/25	**25+19**	**TS4/26**	**26**	**TS-26/27**	**27**	**TS22/26**	**TS24/26**
UMP2[b]	44.5	44.4	50.1	21.1	58.8	9.4	42.1	41.7
(S^2)	(0.796)	(0.761)	(0.967)	(0.927)	(0.777)	(0.893)	(0.913)	(0.803)
PMP2[b]	42.6	43.8	42.9	15.8	57.1	5.6	35.7	39.2
CCSD[b]	49.9	49.4	47.7	19.4	59.5	7.2	42.2	45.3
CCSD(T)[b]	47.5	48.2	44.6	17.6	58.2	6.6	39.6	42.9
ΔH^{298} [c]	47.9	49.3	44.5	18.4	58.8	7.5	39.9	42.9
ΔG^{298} [c]	46.0	37.9	43.9	15.9	56.5	4.3	38.5	42.2
//B3LYP/DZP	*g*	53.7	38.4	14.6	56.0	3.2	41.7	43.9

	28	**TS-28/29**	**29**	**TS-21/29**	**TS-28/30**	**30**	**TS-16/30**
UMP2[b]	18.5	40.3	39.8	41.4	37.2	38.3	42.4
(S^2)	(0.933)	(0.854)	(0.955)	(0.956)	(0.866)	(0.801)	(0.861)
PMP2[b]	12.4	36.5	31.6	33.0	33.1	36.5	39.5
CCSD[b]	17.1	38.1	33.4	34.5	35.9	37.1	39.8
CCSD(T)[b]	15.4	36.7	33.0	33.9	34.6	34.6	37.8
ΔH^{298} [c]	16.1	37.4	33.9	34.4	35.2	35.6	38.1
ΔG^{298} [c]	14.0	34.6	30.5	31.8	32.6	32.9	36.6
//B3LYP/DZP	13.3	30.6	23.9	31.0	29.5	29.1	34.6

	TS-3/31	**31**	**32+19**	**TS-6/6**
UMP2[b]	44.9	12.1	50.9	39.1
(S^2)	(0.951)	(0.901)	(0.761)	(0.765)
PMP2[b]	43.3	7.6	50.3	38.1
CCSD[b]	42.3	9.1	51.1	42.4
CCSD(T)[b]	40.8	8.3	49.1	41.1
ΔH^{298} [c]	41.1	9.3	51.1	40.7
ΔG^{298} [c]	39.2	6.0	37.4	41.0
//B3LYP/DZP	39.9	4.8	47.4	45.2

[a] Corrected for scaled zero-point vibrational energies obtained at the designated level of optimization. [b] Using the DZP basis set and UMP2(fc)/DZP optimized geometries. [c] From relative energies at UCCSD(T)/DZP//UMP2(fc)/DZP including thermal corrections from harmonic frequencies at UMP2(fc)/DZP for $T = 298$K. [d] For the geometry optimized at //UB3LYP/DZP. [e] Optimization starting with the geometry and the force constants from the UMP2(fc)/DZP run converged to a transition state for methyl rotation. [f] Optimization of the MP2(fc)/DZP geometry converged to **16**. [g] Attempts to localize this structure at UB3LYP/DZP were unsuccessful. [h] Optimization of the UMP2(fc)/DZP geometry at UB3LYP/DZP converged to the transition structure corresponding to the C(4)H_2 wagging motion and bearing spin ((C3) 0.53, (C5) 0.61) and charge ((C3) 0.20, (C5) 0.20) distributed equally between C3 and C5.

TABLE 2: NPA[26] Charges[a] and Spin Densities (Italics) Computed at the SCF/DZP//UMP2(fc)/DZP Level of Theory[f] for $[C_6H_{10}]^{\bullet+}$ Stationary Points

	C1	C2	C3	C4	C5	C6		C1	C2	C3	C4	C5	C6
TS-4/14	0.374[b]	0.113	0.229[b]	0.059	0.046	0.179	**TS-23/24**	*1.178*	*−0.153*	*0.035*	*0.015*	*−0.140*	*0.042*
	−0.010	*0.564*	*−0.079*	*0.066*	*−0.142*	*1.225*	**24**	0.139	0.042	0.279[b]	0.481[b]	−0.026	0.084
14	0.073	0.303	0.242	−0.038	0.210	0.210		*1.198*	*−0.146*	*0.008*	*0.005*	*−0.136*	*0.049*
	−0.083	*0.726*	*0.094*	*0.072*	*0.102*	*0.102*	**24**[e]	0.158	0.018	0.689	0.089	−0.020	0.067
TS-14/15	0.104	0.415	0.384	−0.084	0.075	0.105		*1.219*	*−0.154*	*0.011*	*0.009*	*−0.158*	*0.052*
	−0.061	*0.505*	*0.607*	*−0.096*	*0.028*	*0.021*	**TS-16/24**	0.150	−0.116	0.848	0.054	0.012	0.052
TS-14/15*[c]	0.025	0.148	−0.126	0.448	0.010	0.495		*1.188*	*−0.137*	*0.027*	*0.010*	*−0.144*	*0.050*
	−0.015	*0.161*	*−0.220*	*0.619*	*−0.191*	*0.701*	**TS-23/25**	0.161	0.113	0.280	0.100	0.230	0.116
15	0.066	0.284	0.274	−0.036	0.206	0.206		*0.225*	*−0.055*	*0.112*	*0.042*	*−0.176*	*1.029*
	−0.087	*0.741*	*0.076*	*0.087*	*0.100*	*0.100*	**25 + 19**	0.115	0.298	0.115	0.236	0.236	0.000
TS-15/16r	0.072	0.427	−0.053	0.215	0.046	0.292		*0.000*	*0.000*	*0.000*	*0.000*	*0.000*	*1.257*
	−0.062	*0.551*	*−0.185*	*0.952*	*−0.070*	*−0.181*	**TS-4/26**	0.449[b]	−0.026	0.211	0.040	0.076[b]	0.250
TS-15/16i[d]	0.099	0.484	−0.164	0.474	0.005	0.103		*0.315*	*−0.445*	*0.552*	*−0.051*	*−0.181*	*0.947*
	0.024	*−0.196*	*−0.007*	*0.244*	*−0.161*	*1.239*	**26**	0.067	0.291	0.211	0.082	0.132	0.218
16	0.074	−0.017	0.422	0.440	0.043	0.038		*−0.077*	*0.677*	*0.008*	*0.081*	*−0.311*	*0.728*
	0.053	*−0.090*	*0.518*	*0.573*	*0.025*	*−0.099*	**TS-26/27**	0.080	0.223	0.613	0.007	0.060	0.017
TS-16/17	0.065	0.444	−0.077	0.415	0.074	0.078		*0.043*	*−0.111*	*1.118*	*−0.110*	*0.195*	*0.168*
	1.135	*−0.113*	*−0.047*	*0.250*	*0.021*	*−0.041*	**27**	0.089	0.011	0.398	0.109	0.077	0.317
17	0.030	0.467	−0.097	0.443	0.080	0.077		*0.024*	*−0.068*	*0.550*	*0.133*	*−0.283*	*0.762*
	1.187	*−0.077*	*−0.015*	*0.138*	*0.015*	*−0.024*	**TS-22/27**	0.070	0.241	0.160	0.070	0.194	0.267
18+19	0.000	0.471	−0.105	0.471	0.082	0.082		*−0.082*	*0.744*	*−0.151*	*−0.075*	*0.894*	*−0.352*
	1.257	*0.000*	*0.000*	*0.000*	*0.000*	*0.000*	**TS-24/26**	0.118	0.440	0.037	0.126	0.174	0.105
TS-4/20	0.078	−0.022	0.050	0.101	0.087	0.707		*0.032*	*−0.195*	*0.365*	*−0.031*	*−0.091*	*1.048*
	0.951	*−0.704*	*0.930*	*−0.119*	*0.034*	*0.088*	**28**	0.065	0.276	0.169	0.101	0.149	0.241
20	0.245	0.230	0.027	0.190	0.208	0.100		*−0.078*	*0.698*	*−0.105*	*0.099*	*−0.310*	*0.810*
	0.891	*−0.236*	*0.257*	*0.023*	*0.179*	*−0.007*	**TS-28/29**	0.029	0.207	0.089	0.483	−0.066	0.259
TS-16/20	0.445	−0.040	0.444	0.113	−0.059	0.097		*−0.129*	*1.058*	*−0.197*	*0.233*	*−0.313*	*0.376*
	−0.360	*0.051*	*0.430*	*1.126*	*−0.167*	*0.045*	**TS-21/29**	0.132	0.710	0.003	0.099	−0.003	0.058
TS-20/21	0.059	0.004	0.107	0.000	0.694	0.135		*0.002*	*0.016*	*−0.104*	*0.981*	*−0.714*	*0.966*
	0.961	*−0.715*	*0.981*	*−0.108*	*0.017*	*−0.000*	**29**	0.146	0.690	0.047	0.059	−0.013	0.071
21	0.047	0.397	0.397	0.047	0.068	0.044		*0.001*	*0.024*	*−0.094*	*0.957*	*−0.713*	*0.974*
	−0.098	*0.545*	*0.545*	*−0.098*	*0.024*	*0.006*	**TS-28/30**	0.055	0.251	−0.102	0.260	0.308	0.229
TS-16/21	0.304	0.196	0.282	0.094	0.062	0.062		*−0.040*	*0.379*	*−0.293*	*0.226*	*−0.225*	*1.029*
	−0.109	*1.111*	*−0.107*	*0.043*	*0.045*	*0.004*	**30**[d]	0.092	0.506	−0.164	0.466	−0.003	0.103
TS-16/22	0.430[b]	0.051	0.160	0.214[b]	0.060	0.086		*0.084*	*−0.111*	*−0.054*	*0.214*	*−0.157*	*1.107*
	0.026	*−0.144*	*1.176*	*−0.145*	*0.081*	*−0.002*	**TS-16/30**	0.118	0.537	−0.106	0.335	0.001	0.114
TS-21/22	0.745[b]	−0.060[b]	0.161	0.031	−0.006	0.129		*0.010*	*−0.120*	*−0.159*	*0.375*	*−0.173*	*1.144*
	0.068	*−0.148*	*1.170*	*−0.154*	*0.005*	*0.007*	**TS-3/31**	0.082	0.001	0.057	0.209	0.186	0.464
22	0.374	0.025	0.138	0.030	0.176	0.257		*0.971*	*−0.697*	*0.925*	*−0.875*	*0.008*	*0.032*
	0.007	*−0.147*	*1.196*	*−0.145*	*0.010*	*0.006*	**31**	0.459	−0.055	0.132	0.400	0.006	0.057
TS-22/23	0.721	−0.004	0.177	0.027	−0.035	0.114		*0.793*	*−0.307*	*0.175*	*0.504*	*−0.063*	*0.027*
	0.043	*−0.152*	*1.172*	*−0.148*	*0.028*	*0.015*	**32 + 19**	0.416	−0.121	0.415	−0.128	0.418	0.000
23	0.364	0.079	0.395	0.058	0.025	0.079		*0.000*	*0.000*	*0.000*	*0.000*	*0.000*	*1.258*
	0.657	*−0.208*	*0.593*	*−0.040*	*−0.058*	*0.057*	**TS-6/6**	0.124[b]	0.597	0.124[b]	0.059	0.037	0.059
TS-23/24	0.167	−0.003	0.730	0.048	0.003	0.055		*−0.128*	*1.177*	*−0.128*	*0.046*	*0.002*	*0.046*

[a] Hydrogen charges were summed into carbon atoms. [b] The charge of the migrating hydrogen was split equally. [c] UHF/6-31G*//UHF/6-31G*. [d] UHF/DZP//UB3LYP/DZP. [e] UHF/6-31G*//UMP2(fc)/6-31G*. [f] If not stated otherwise.

a [1,2]-hydrogen migration leading to a methylenecyclopentane radical cation, **12**.[14] Isomerization of the latter to 1-methylcyclopentene radical cation, **13**, (the most stable $[C_6H_{10}]^{\bullet+}$ isomer we found) involves a [1,3]-H shift with an activation energy of 42.2 kcal mol^{-1} (relative to **12**). In addition to that, methyl radical loss from **13** would primarily generate an open shell $[C_5H_7]^+$ species probably too high in energy to explain the experimental observation.

Hydrogen shifts to form a terminal methyl group may also occur in acyclic $[C_6H_{10}]^{\bullet+}$ intermediates formed by addition of ethylene to the butadiene radical cation. Subsequent cyclization to five membered rings rather than to the cyclohexene radical cation, **6**, might then occur. [1,4]-, [1,5]- and [1,6]-hydrogen shifts were all claimed by Bouchoux and Salpin to occur readily in $[C_6H_{10}]^{\bullet+}$ because they are "known to be facile processes with critical energies below 10 kcal mol^{-1} in radical and cation−radical chemistry".[12] Reaction paths **F**, **G**, and **H**, discussed below start with a [1,4]-, a [1,2]- and a [1,5]-H shift, respectively, in the distonic intermediate **4**. The activation barriers ($\Delta E^{\ddagger}$) are 33.8, 10.0, and 7.7 kcal mol^{-1}, respectively (Chart 1). The search for a [1,3]-H shift lead to path **I** which accounts for a direct hydrogen exchange reaction between **1** and **2** without the involvement of **4**. Different subsequent pathways have been labeled with additional lowercase letters (**Fa**, **Fb**, etc.).

I. Path F ([1,4]-Hydrogen Shift). The addition reaction of ethylene, **1**, to the butadiene radical cation, **2**, via an ion−molecule complex to form an open-chain distonic intermediate, **4**, (Chart 1) occurs very easily (no barrier for ΔE, activation free energy $\Delta G^{298\ddagger}$ of 2.7 kcal mol^{-1}).[14]

A [1,4]-hydrogen shift from C4 to C1 in **4** generates a methyl group at C1 and moves the allyl cation moiety from C1−C2−C3 to C2−C3−C4. The transition structure, **TS-4/14** (Figure 1), reveals that while the radical center is located on C6, the [1,4]-hydrogen shift essentially resembles that of the butenyl cation (a thermally allowed antarafacial sigmatropic shift). The barrier relative to **4** is 33.8 kcal mol^{-1} (34.7 kcal mol^{-1} at ΔG^{298}) which compares to a value of 33.0 kcal mol^{-1} for the butenyl cation case (at the same level). The approaching spin and charge centers result in a ring closure to the methylvinyl cyclopropane radical cation **14**, as a step coupled with the H-shift. Vinyl cyclopropane radical cations can rearrange into cyclopentenes

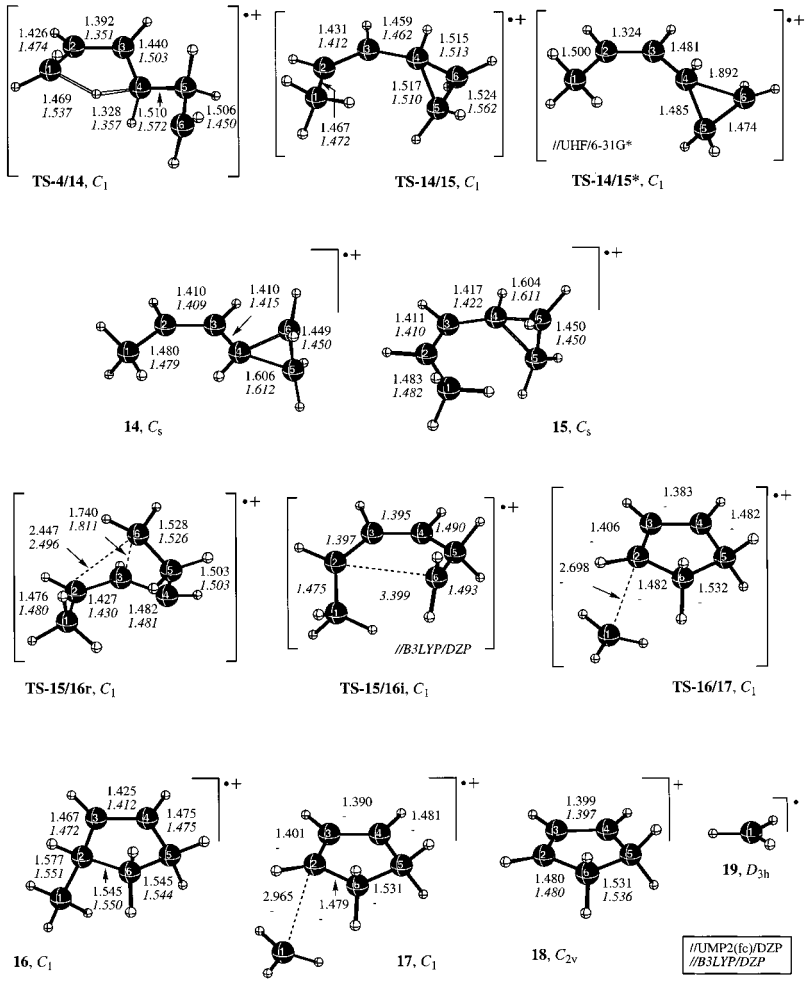

Figure 1. Optimized $[C_6H_{10}]^{\bullet+}$ geometries of structures relevant for path **F**: [1,4]-hydrogen shift and vinylcyclopropane/cyclopentene rearrangement.

CHART 1: The Initial Steps for Paths F, G, and H in Comparison: [1,4]-, [1,2]- and [1,5]-Hydrogen Shifts, Respectively, in 4

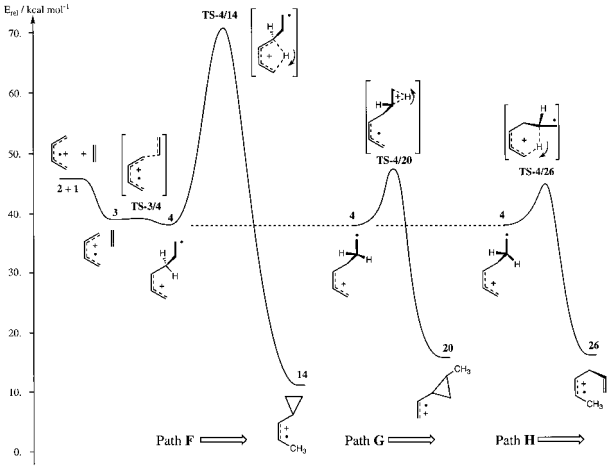

relatively easily (compared to the neutral reaction) by [1,3]-alkyl shifts.[27] For example, Dinnocenzo and Conlon[28] experimentally observed a strong acceleration of the vinylcyclopropane to cyclopentene rearrangement upon one-electron oxidation in 1988. Though ring expansion to a five membered ring is prevented in **14** by the *exo* orientation of the methylvinyl group, it is possible after conversion to the *endo* isomer, **15**. While the oxidized double bond in **14** and **15** is stabilized by hyperconjugative interaction with the cyclopropyl group, this is not possible in the rotational transition structure **TS-14/15**, because of the unfavorable orientation of the π-system relative to the cyclopropenyl group. This gives rise to a relatively large 17.3 kcal mol^{-1} rotational barrier. As in the vinylcyclobutane case (compare **TS-8/10**), in **TS-14/15** the electron is missing from the C−C π-bond. The electronically excited rotational transition state **TS-14/15*** with the "hole" located in a cyclopropyl C−C σ-bond is 8.8 kcal mol^{-1} higher in energy at UHF/6-31G* and was not optimized at higher levels of theory. The ring expansion from **15** (which is 5.2 kcal mol^{-1} less stable than **14**) to the 3-methyl cyclopentenyl radical cation, **16**, may proceed with retention (path Fa) or with inversion of the C(6)-H_2 methylene group (path Fb). For the concerted rearrangement of the parent vinylcyclopropane radical cation, inversion ($E_{rel}^{\ddagger}$ = 21.3 kcal mol^{-1}) was shown to be preferred over retention ($E_{rel}^{\ddagger}$ = 30.9 kcal mol^{-1}).[27] For the methyl derivative **15**, the transition state for methylene inversion (**TS-15/16i**, $E_{rel}^{\ddagger}$ = 19.6 kcal mol^{-1} vs **15**) is 9.2 kcal mol^{-1} lower in energy than that for methylene retention (**TS-15/16r**, $E_{rel}^{\ddagger}$ = 28.8 kcal mol^{-1}). Similar to the parent rearrangement, the inversion transition state **TS-15/16i** can be described with a radical center (located at C6) and an allyl cation moiety. We were able to locate **TS-15/16i** only at the UB3LYP/DZP but not at the UMP2/DZP level. For the parent vinylcyclopropane radical cation the barriers for a stepwise and for the concerted rearrangement with inversion are essentially equally high.[27] The stepwise alternative was not further investigated here. The important point is that the methylvinylcyclopropane radical cation, **15**, was shown to rearrange to methylcyclopropene radical cation, **16**, below the

CHART 2: Reaction Pathway F Which Connects Ethylene and the Butadiene Radical Cation with the Cyclopentene Cation plus Methyl Radical through a [1,4]-hydrogen Shift in the Acyclic Distonic Intermediate, 4, Leading to the Methylvinylcyclopropane Radical Cations 14 and 15

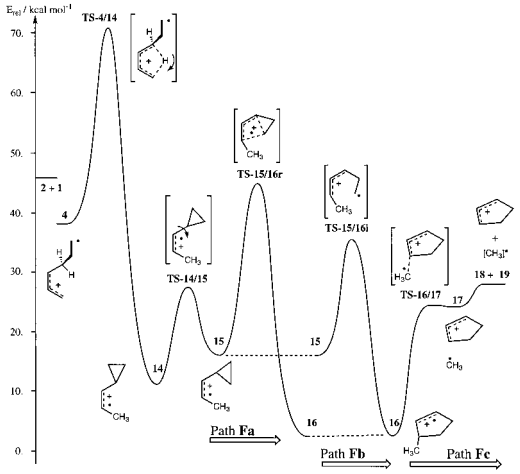

CHART 3: Reaction Pathway G Leading to the Methylcyclopentene Radical Cations 16 and 21 via a [1,2]-hydrogen Shift in 4 and Ring Expansion of the Intermediate Vinylmethylcyclopropane Radical Cation, 20

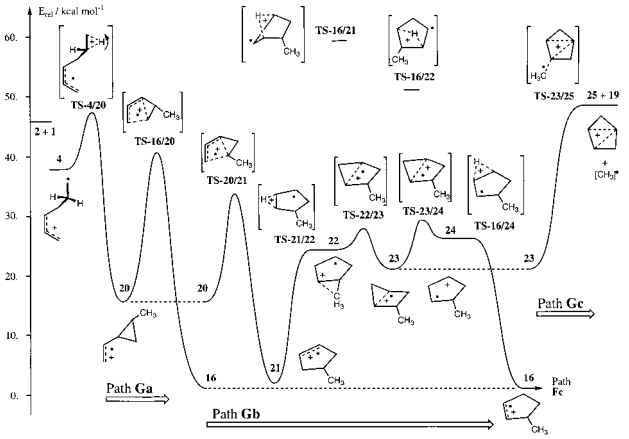

energy limit of the initial complex between the butadiene radical cation and ethene. However, the critical step along this path (**F**) is clearly the initial [1,4]-hydrogen shift (compare Chart 2). The dissociation of **16** into the cyclopentenyl cation, **18**, and methyl radical fragments **19** (path **Fc**) is endothermic (ΔH^{298}) by 25.3 kcal mol^{-1} (15.9 kcal mol^{-1} at ΔG^{298}) proceeding via **TS-16/17** and an ion-molecule complex, **17**, which both are a little lower in energy on the potential energy surface than separated **18** and **19**. Considering ΔG^{298} values, however, **TS-16/17** is 4.5 kcal mol^{-1} higher in energy than **18** + **19**, giving rise to a small barrier for the reverse reaction (addition of **18** and **19**). Fragmentation into $[C_5H_7]^+$ and $[CH_3]^\bullet$ is unlikely to occur in the condensed phase where (vibrationally excited) low energy intermediates (**14**−**16**) can be deactivated by collisions, but in the gas phase under low-pressure conditions methyl loss is a way to dissipate the excess energy.

II. Path G ([1,2]-Hydrogen Shift). A transition state search for a [1,2]-hydrogen shift in the distonic radical cation **4** to move the radical center from the C6 to the C5 position converged to **TS-4/20** (Figure 2) which is predicted to lie 10.0 kcal mol^{-1} higher in energy than **4**. It was confirmed by IRC computations

CHART 4: Reaction Pathways Following a [1,5]-hydrogen Shift in the Distonic Intermediate 4 (Path H Leading to the 2-Methylcyclopentene Radical Cation)

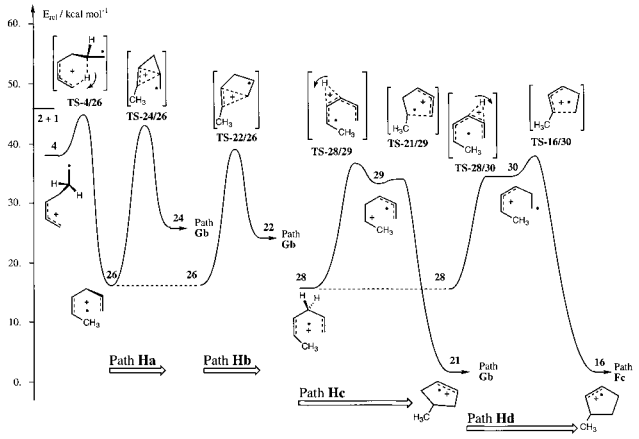

CHART 5: The Coupled H-shift/Addition Reaction between Ethylene, 2, and the butadiene Radical, 1 (Path I)

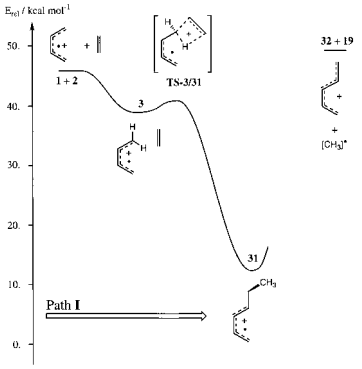

to connect minima **4** and **20**, a methylated vinyl cyclopropane radical cation. Hence, a C3−C5 cyclopropyl ring closure is coupled with the [1,2]-H shift. According to the computed charges and spin densities (Table 2), in **TS-4/20** a hydrogen migrates to a C6 cationic center while the C1−C2−C3 π-system holds the unpaired electron.

As **20** has an *endo* oriented vinyl group (see Figure 2) it can directly ring expand to either 4- (**21**) or 3-methylcyclopropene radical cation, **16**, by breaking the C3−C5 (path **Ga**) or the C3−C4 bond (path **Gb**), respectively. Breaking C3−C5 generates a secondary carbon at C5, but breaking C3−C4 generates a primary C4 carbon atom. The positive charge has a greater preference for the allyl over the *primary* alkyl position than the radical. However, this is reversed for allyl and a *secondary* alkyl position as can be seen from the equations in Scheme 3. Therefore, in the first case, the transition state **TS-20/21** has essentially a (secondary) carbocation center at C5 and a C1−C2−C3 allyl radical moiety. In the second case, however, C4 in **TS-16/20** holds the unpaired electron and the positive charge is located in the allyl moiety. Formation of **21**, via **TS-20/21** with an activation of 18.6 kcal mol^{-1} is favored (by 6.5 kcal mol^{-1}) over the direct rearrangement of **20** to **16**. This is only slightly less than for the concerted inversion rearrangement from **15** to **16** (19.6 kcal mol^{-1}) where the methyl group is attached to the vinyl rather than to the cyclopropyl moiety. For the parent $[C_5H_8]^{\bullet+}$ radical cation the barrier for the vinylcyclopropane to cylopentene rearrangement is predicted to be 21.3 kcal mol^{-1}.[27]

The methyl group in **20** stabilizes the positive partial charge at C5 and allows enhanced hyperconjugative interaction with

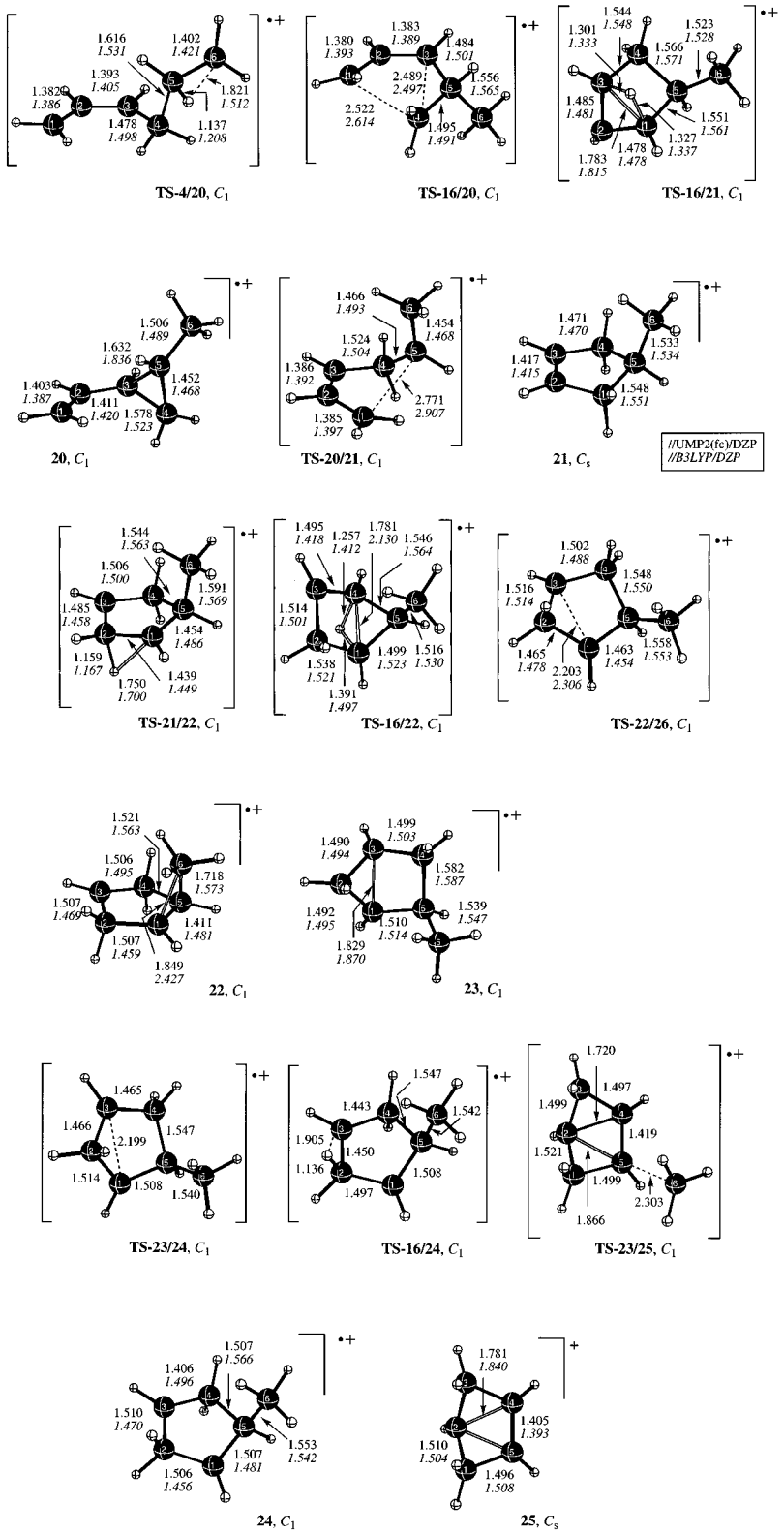

Figure 2. Optimized $[C_6H_{10}]^{\bullet+}$ geometries involved in the [1,2]-hydrogen shift and vinylcyclopropane/cyclopentene rearrangement (path **G**).

the π-system resulting in a longer C3−C5 bond (1.632 Å compared to 1.578 Å for C3−C4). This might also explain why breaking the (weakened) C3−C5 bond is preferred over C3−C4 breaking. A [1,3]-hydrogen shift could transform the preferred rearrangement product, **21**, to **16** which was shown above to lose methyl relatively easily (compare Path **Fc**). In the transition structure, **TS-16/21**, which connects **16** and **21** through a single [1,3]-H shift, C2 becomes a radical center and the migrating hydrogen is bound to C1 and C3 by a three center two electron bond. However, for this step we compute a large barrier of 59.6 kcal mol^{-1} (Chart 2). The predicted barrier for the parent cyclopentene radical cation is almost identical: 59.0 kcal mol^{-1}.[29]

As an alternative to a [1,3]-H shift, a [1,2]-H shift can also occur. This separates spin and charge into 1,3 positions. A hydrogen can move from C1 to C2 in **21** formally as a hydride or as a proton, which generates the carbocation center at C1 (**22**) and C3 (**24**), respectively, and the radical center at C3 (**22**)

SCHEME 3

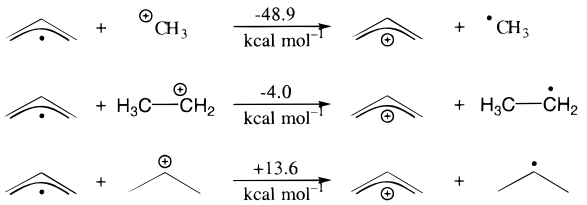

UCCSD(T)/DZP//MP2(fc)/DZP + 0.93 ZPE(UMP2(fc)/DZP)

and C1 (**24**), respectively. Localization of the charge in the alpha position relative to the methyl substituted C5 at C1 together with the unpaired electron at C3 (see Figure 2), **22**, (E_{rel} = 24.3 kcal mol^{-1}) is slightly favored over the alternative (radical at C1 and charge at C3), **24** (E_{rel} = 26.6 kcal mol^{-1}) because of hyperconjugative stabilization of the C1 carbenium center by the C5−CH_3 bond in **22**. The structure of **22** is described as classical at the HF and B3LYP levels, but as methyl bridged at the MP2/6-31G* and MP2/DZP levels. Likewise there is a qualitative change for the **24** structure, which is classical from the HF/6-31G*, MP2/6-31G* and B3LYP/DZP optimizations, but hydrogen bridged between C4 and the cationic C3 at the MP2/DZP level. Higher level single points with the DZP basis set reduce the preference for the H-bridged structure from 1.9 kcal mol^{-1} at UMP2/DZP to 0.3 kcal mol^{-1} at UCCSD(T)/DZP. Transition structure **TS-21/22**, connects **21** to **22**, but at our best level, **TS-21/22** and **22** are equal in energy (and **TS-16/24** becomes even lower in energy than **24**, see below). This suggests that the distonic intermediates **22** and **24** readily collapse to the more stable methylcyclopentene radical cations **21** and **16**, respectively, by [1,2]-H shifts without a barrier. It should be added, that **21**, **22**, and **24** can probably undergo further [1,2]-hydrogen shift isomerizations easily, e.g., to **13** but this is likely not to lose a methyl radical as easily as **16**. A [1,3]-H shift transforms **22** into **16**, but the corresponding transition structure, **TS-16/22** is 51.2 kcal mol^{-1} high in energy. However, **22** and **24** can interconvert through the slightly more stable (3.2 kcal mol^{-1} vs **22**) 2-methylbicyclo[2.1.0]pentane radical cation, **23** (formation of a transannular one-electron bond). The transition structures involved, **TS-22/23** and **TS-23/24**, are only 4.0 and 2.9 kcal mol^{-1} higher in energy than **22** and **24**, respectively. A bicyclo[2.1.0]pentane radical cation was not detected experimentally when 1,3-pentadiene was oxidized in matrix, but it was observed by radiolytic oxidation of bicyclo[2.1.0]pentane (in Freon matrixes at 77 K) and was found to isomerize easily to the cyclopentene radical cation (at ca. 100 K).[30]

Breaking the transannular one-electron bond in **23** requires only very small activation and produces a distonic 1,3-cyclopentadiyl structure **22** or **24**. A [1,2]-hydrogen shift in **24** leads to **16** with a low activation of 0.8 kcal mol^{-1} at MP2/DZP; and from CCSD(T)/DZP single points, the transition structure, **TS-16/24** is even lower in energy than **24** by 1.0 kcal mol^{-1}. On the other hand the [1,3]-H shift leading from **22** to **16** has a high barrier of 26.9 kcal mol^{-1}. The latter findings are in accordance with experiments on bridgehead methylated bicyclo[2.1.0]pentanes:[31] one-electron oxidation (photoinduced electron transfer or radiolytic oxidation) of the mono methylated derivative gives the 3-methylcyclopentene radical cation (thermodynamically less stable than the 1-methyl isomer). This is presumably generated by a [1,2]-H shift to the methylated cationic center of an intermediate 1,3-diyl structure but no intermediate was located in this case (Scheme 4). Bridgehead

SCHEME 4

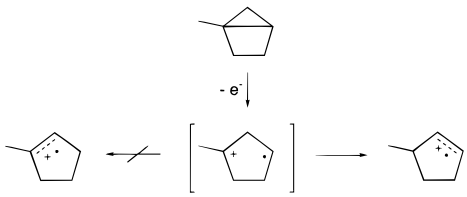

bismethylation leads to more persistency and an intermediate could be observed by ESR.[31]

Direct methyl loss of **23** is endotherm by 27.1 kcal mol^{-1} and leads to a $[C_5H_7]^+$ species with a bishomocyclopropenyl cation structure, **25**. The latter is 20.5 kcal mol^{-1} higher in energy than the cyclopropenylium cation, **18**. This brings **25** very close to the upper possible limit (21.5 kcal mol^{-1} relative to **18**)[32] estimated by Bouchoux and Salpin.[12] The hydrogen shift to convert **25** into **18**, the postulated[12] structure of the mass spectrometrically observed $[C_5H_7]^+$, has a barrier of only 3.2 kcal mol^{-1}, but **25** does not seem to be important because **18** may be formed more easily via **16** (see below).

We tried to localize the transition structure for direct methyl loss of **21** but did not succeed. A series of partial optimizations at UB3LYP/6-31G* with fixed C5−C6 distances elongated in 0.1 Å steps up to 2.80 Å gave continuously increasing energies. We therefore conclude that most likely no transition structure is involved in the dissociation of **21** into a methyl radical and the cyclopentene-4-yl cation, which together have a relative energy of 50.7 kcal mol^{-1}. A [1,2]-H shift to bring the cyclopentenyl carbocation center from position 4 to position 3 in conjugation with the double bond is a very easy process.

We did not try to find transition structures for methyl loss from **22** or from **24**, because we could show that methyl loss from **23** via transition structure **TS-23/25** does not require extra activation over the relative energy of **25** + **19**. In other words the back reaction **25** + **19** → **23** is essentially barrierless. (At UMP2/DZP **TS-23/25** is only 0.1 kcal mol^{-1} higher in energy than **25** + **19** and at our highest level it becomes even a little more stable.)

III. Path H ([1,5]-Hydrogen Shift). A [1,5]-hydrogen shift from C5 to C1 in **4** creates the 1,4-hexadiene radical cation, **26**, with two ene moieties (C2−C3 and C5−C6 according to the numbering in Figure 3) separated by a methylene group (C4). Intermediate **26** can undergo ring closure by an intramolecular [2+1] cycloaddition. Transitions structures **TS-22/26** and **TS-24/26** have relative energies of only 39.6 and 42.9 kcal mol^{-1}, respectively, and have been confirmed by IRC computations to connect **26** with the methylcyclopenta-1,3-diyl structures **22** and **24**, respectively. Both **22** and **24** can isomerize to **16** (path **Gb**), which can loose a methyl radical easily (path **Fc**). For the hole catalyzed intramolecular ene dimerization of 1,4-pentadiene we compute a 23.8 kcal mol^{-1} barrier and a small exothermicity of 1.1 kcal mol^{-1} to the bicyclo[2.1.0]pentane radical cation.[27] The analogous reaction of the methylated **26** requires an activation of 25.3 kcal mol^{-1} and leads to the distonic **22**, which easily isomerizes further to **16** (see path **Gb**). For the intermolecular [2+1] addition of ethylene plus ethylene radical cation to give the cyclobutane radical cation, Jungwirth and Bally computed a barrier of 9.0 kcal mol^{-1} and an energy change of −22.4 kcal mol^{-1} (QCISD(T)/6-31G*//UMP2/6-31G*).[33] The intramolecular reactions of the 1,4-pentadiene radical cation and of **26** are less favorable due to the additional ring strain built up in the bicyclic products.

Various conformational changes of the 1,4-hexadiene radical cation should be very easy as long as they correspond to C−C

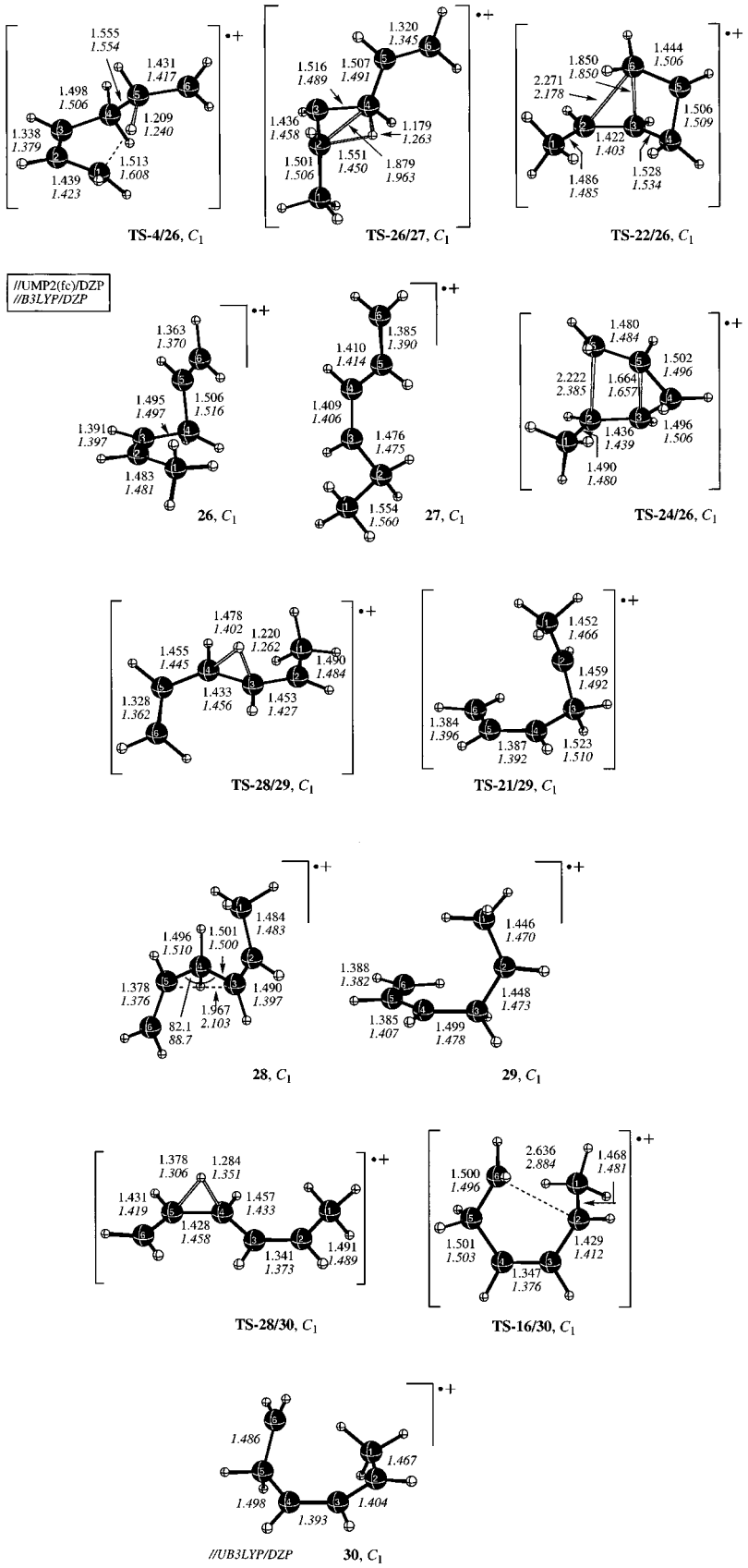

Figure 3. Optimized geometries important for path **H** starting with the [1,4]-hydrogen shift in intermediate **4** and for some side reactions.

single bond rotations. While in **26** the two ene moieties are favorably oriented for a cyclization, they point in opposite directions in conformer **28**, which is 2.2 kcal mol^{-1} lower in energy than **26**. As an alternative to immediate cyclization (paths **Ha** and **Hb**), **26** or **28** may undergo further H-shift reactions. A [1,3]-hydrogen shift (from C4 to C2) could transform **26** to a 1,3-hexadiene radical cation, **27**, which has a relative energy $E_{rel} = 6.6$ kcal mol^{-1}, but the corresponding transition structure

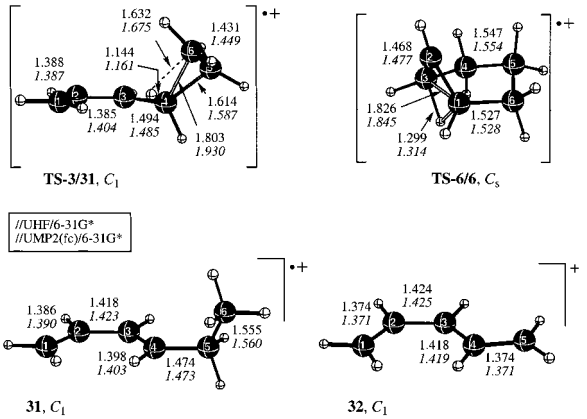

Figure 4. Optimized geometries for path **I**: simultaneous H-shift and addition reaction between ethylene, **1**, and the *cis*-butadiene radical cation, **2**.

TS-26/27 is quite high in energy: $E_{rel} = 58.2$ kcal mol^{-1}. We did not search for the transition state for the [1,3]-H shift leading to the 2,4-hexadiene radical cation, but this can be surmised to be very high in energy, as well. A [1,2]-H shift can move one methylene (C4) hydrogen in **28** to C3 (path **Hc**) or C5 (path **Hd**). In the first case, the distonic intermediate **29** has an allyl moiety (C4−C5−C6) and a secondary carbocation center (C2). In contrast, the allyl moiety in **30** (C2−C3−C4) holds the charge and the unpaired electron is located at the primary C6 position. These correspond to the preferred combinations according to the equations in Scheme 3. Structure **29** ($E_{rel} = 33.0$ kcal mol^{-1}) is only slightly lower in energy than **30** ($E_{rel} = 34.6$ kcal mol^{-1}). The latter could only be located at the B3LYP/DZP level. (The HF/6-31G* optimization converged to **20**.) Ring closure of **29** and **30** result in **21** and **16**, respectively. As shown above, **21** can isomerize to **16** (path **Gb**) and **16** loses a methyl radical easily (path **Fc**). The transition structures **TS-21/29** and **TS-16/30** are only 0.9 and 3.2 kcal mol^{-1} higher in energy than **29** and **30**, respectively. We did not confirm by IRC calculations that **TS-28/29**, **TS-21/29**, **TS-28/30** and **TS-16/30** connect to the conformations chosen for **28**, **29** and **30**. However, conformational changes should be easy compared to the rearrangement reactions.

IV. Path I ([1,3]-Hydrogen Shift). The search for a transition state for the [1,3]-hydrogen shift from C4 to C6 in **4** to give a 1,3-hexadiene radical cation, led to **TS-3/31** (Figure 4). The vector of its (only) imaginary vibrational frequency (342i cm^{-1}) corresponds to a hydrogen moving from C4 to C6 (or from C6 to C4). Following the IRC, however, revealed that **TS-3/31** connects the 1,3-hexadiene radical cation conformer **31** with the complex **3** and not with the distonic intermediate **4**. Thus, addition of **1** to **2** and a hydrogen transfer can occur simultaneously. Theoretical spin densities show that in **TS-3/31**, C1−C2−C3 forms essentially an allyl radical moiety and the reaction step can be described as a C−H addition of a C4 cationic center to the C5−C6 double bond. The barrier for this coupled H-shift/addition step involving **TS-3/31** is computed to be only 3.9 kcal mol^{-1}. This situation parallels the findings of Jungwirth and Bally that the 1-butene radical cation is connected to a complex between ethylene and the ethylene radical cation by a low-lying transition structure for H-shift and addition with a small barrier of 5.9 kcal mol^{-1}.[33] Intermediate **31** has enough excess energy to overcome the 32.5 kcal mol^{-1} barrier for the **31** → **3** back reaction as long as it is not deactivated. By a back and forth reaction **3** → **31** → **3**, ethylene, **1**, and the butadiene radical cation, **2**, can exchange all their methylene hydrogens (one at a time). Hydrogen scrambling preceding methyl radical loss was observed experimentally under low-pressure conditions.[12]

Methyl radical loss of **31** gives the pentadienyl cation, **32**, predicted to lie 21.4 kcal mol^{-1} higher in energy than the cyclic $[C_5H_7]^+$ isomer, **18**, which makes the overall reaction **1** + **2** → **32** + **19** endothermic by 3.5 kcal mol^{-1} (3.9 kcal mol^{-1} at ΔG^{298}). This pathway seems of less importance compared to the alternatives discussed above and we did not try to locate the transition state between **31** and **32** + **19** (or a complex of both).

V. [1,3]-Hydrogen Shifts. Derrick et al. reported from their experiment that the dissociation of field ionized deuterated cylohexene is preceded by randomization of hydrogen and deuterium atoms.[13] It was also proposed that this is due to successive 1,3-allylic rearrangements. We computed the transition structure **TS-6/6** for [1,3]-hydrogen shift in the cyclohexene radical cation, **6**, and found the barrier to be very high: 41.1 kcal mol^{-1}. But this is not in contradiction to the experimental observation, because the radical cations are generated with an energy excess of ca. 69 kcal mol^{-1} (3 eV). (The ionization potential of cyclohexene is 8.945 ± 0.01 eV,[34] and the ionization was carried out by electron impact with an energy of nominally ca. 12 eV. The analogous [1,3]-hydrogen shift in the cyclopentenyl radical cation requires an even higher activation of 59.0 kcal mol^{-1}.[27] The [1,3]-H shift in the propene radical cation, the simplest model for this type of reaction, has been investigated with ab initio methods by Clark.[35] He predicted a 29.6 kcal mol^{-1} barrier for the suprafacial [1,3]-H shift at UMP2/6-31G*//UHF/6-31G*. At the MP2 level the process is described as two consecutive [1,2]-shifts, since the C_s structure is a shallow minimum instead of a transition structure; but this may be an artifact of the method.[36] Nguyen et al. reported that for the radical cation the rearrangement occurs via an antarafacial pathway with a C_s transition structure involving a hydride transfer.[37] In contrast, the process in neutral propene has a C_2 transition structure and a migrating proton. They found the barriers to be 33.2 and 85.6 kcal mol^{-1} for the ionized and neutral propene, respectively (at spin projected MP4/6-31G(d,p)//UMP2(fc)/6-31G(d,p) including ZPE corrections from UHF/6-31G(d,p) results). The increased barriers (relative to 33.2 kcal mol^{-1} for the propene radical cation) for the cyclic molecules (41.1 kcal mol^{-1} for the cyclohexene radical cation and 59.0 kcal mol^{-1} for the cyclopentene radical cation) are due to the additional strain in the transition structures where the carbon atoms exchanging one hydrogen atom must come relatively close (1.826 Å in **TS-6/6**, compare Figure 4).

Conclusions

We have presented a detailed study of the $[C_6H_{10}]^{\bullet+}$ potential energy surface focusing on reaction pathways including H-shift reactions and thus complementing our earlier study on reactions leading from the butadiene radical cation and ethylene to the cyclohexadiene radical cation.[14] For the [1,2]- (10.0 kcal mol^{-1}, **TS-4/20**) and [1,5]-hydrogen shifts (7.7 kcal mol^{-1}, **TS-4/26**) we find low activation energies, while the [1,4]- (33.8 kcal mol^{-1}, **TS-4/14**) and [1,3]-H shifts (e.g. 42.2 kcal mol^{-1}, **TS-12/13**; 57.2 kcal mol^{-1}, **TS-16/21**; 48.8 kcal mol^{-1}, **TS-16/22**) are characterized by large barriers.

The formation of a cyclopentadienyl cation $[C_5H_7]^+$, **18**, from **1** + **2** (under methyl radical loss) as observed in experimental mass spectrometric investigations[12] is likely not to origin from just one single pathway because many rearrangement reactions have been found to occur below the energy of the separated

reactants. The following reaction sequence is the most straightforward route from **1** + **2** to **18** + methyl radical, **19**, through the transition structures lowest in energy: (i) addition of **2** to **1** leading to a distonic open-chain intermediate, **4**. (ii) [1,5]-hydrogen shift from **4** to give the 1,4-hexadiene radical cation, **22**, (path **H**). (iii) further intramolecular [2+1] cycloaddition leading to 4-methyl-cyclopenta-1,3-diyl structure, **22** (path **Hb**) which can easily convert into **24** via 2-methyl-bicyclo[2.1.0]-pentane radical cation, **23**. (iv) [1,2]-H shift of **24** to 3-methyl-cyclopentene radical cation, **16**, (path **Gb**). (v) methyl radical loss (path **Fc**). This reaction sequence involves only transition structures lower in energy (ΔE) than **1** + **2**. The transition state for the [1,5]-H shift, **TS-4/26**, has the largest ΔG^{298}, 10.4 kcal mol^{-1} higher than that for **1** + **2**.

Hydrogen exchange between **1** and **2** can also occur via a concerted hydrogen transfer/ addition reaction leading to a 1,3-hexadiene intermediate, methyl radical loss from which is disfavored relative to back dissociation into **1** and **2**.

Acknowledgment. This research was supported by the U.S. Department of Energy, Office of Basic Energy Sciences, Fundamental Interactions Branch, Grant DOE-FG02-97ER14748. M.H. gratefully acknowledges a postdoctoral fellowship by the DAAD. We thank a referee for helpful suggestions.

Supporting Information Available: Tables of absolute energies and Cartesian coordinates of various stationary points on the $[C_6H_{10}]^{\bullet+}$ potential energy surface. Supporting Information is available free of charge via the Internet at http://pubs.acs.org.

References and Notes

(1) Houk, K. N. *Acc. Chem. Res*. **1975**, *8*, 361.
(2) Müller, F.; Mattay, J. *Chem. Rev.* **1993**, *93*, 99.
(3) Bauld, N. L. *J. Am. Chem. Soc.* **1992**, *114*, 5800.
(4) Schmittel, M.; Wöhrle, C.; Bohn, I. *Chem. Eur. J.* **1996**, *2*, 1031.
(5) Hintz, S.; Heidbreder, A.; Mattay, J. *Top. Curr. Chem.* **1996**, *177*, 77.
(6) For a review see: Bauld, N. L. *Tetrahedron* **1989**, *45*, 5307.
(7) Schmittel, M.; von Seggern, H. *Angew. Chem.* **1991**, *103*, 981.
(8) Schmittel, M.; von Seggern, H. *J. Am. Chem. Soc.* **1993**, *115*, 2165.
(9) (a) Schmittel, M.; Wöhrle, C. *Tetrahedron Lett.* **1993**, *34*, 8431. (b) Schmittel, M.; Wöhrle, C. *J. Org. Chem.* **1995**, *60*, 8223.
(10) Woodward, R. B.; Hoffmann, R. *Angew. Chem.* **1969**, *81*, 797; *Angew. Chem., Int. Ed. Engl.* **1969**, *8*, 781.
(11) Fleming, I. *Frontier Orbitals and Organic Chemical Reactions*; New York 1977.
(12) Bouchoux, G.; Salpin, J.-Y. *Rapid Commun. Mass Spectrom.* **1994**, *8*, 325.
(13) Derrick, P. J.; Fallick, A. M.; Burlingame, A. L. *J. Am. Chem. Soc.* **1972**, *94*, 6794.
(14) Hofmann, M.; Schaefer, H. F. *J. Am. Chem. Soc.* **1999**, *122*, 6719. Also see: ref 15.
(15) Haberl, U.; Wiest, O.; Steckhan, E. *J. Am. Chem. Soc.*, **1999**, *121*, 6730.
(16) Frey, H. M.; Pottinger, R. *J. Chem. Soc., Faraday Trans. 1* **1978**, 1827.
(17) Sastry, G. N.; Bally, T.; Hrouda, V.; Cársky, P. *J. Am. Chem. Soc.* **1998**, *120*, 9323.
(18) M. J. Frisch, G. W. Trucks, H. B. Schlegel, P. M. W. Gill, B. G. Johnson, M. A. Robb, J. R. Cheeseman, T. Keith, G. A. Petersson, J. A. Montgomery, K. Raghavachari, M. A. Al-Laham, V. G. Zakrzewski, J. V. Ortiz, J. B. Foresman, J. Cioslowski, B. B. Stefanov, A. Nanayakkara, M. Challacombe, C. Y. Peng, P. Y. Ayala, W. Chen, M. W. Wong, J. L. Andres, E. S. Replogle, R. Gomperts, R. L. Martin, D. J. Fox, J. S. Binkley, D. J. Defrees, J. Baker, J. P. Stewart, M. Head-Gordon, C. Gonzalez, J. A. Pople, *Gaussian 94*, Revision C.3; Gaussian, Inc., Pittsburgh, PA, 1995.
(19) (a) Huzinaga, S. *J. Chem. Phys*. **1965**, *42*, 1293. (b) Dunning, T. H. *J. Chem. Phys.* **1970**, *53*, 2823.
(20) The use of DZP instead of 6-31G* may not be worth the additional costs, at least in cases where hydrogen atoms are not directly involved in the reaction. For hydrogen shift transition structures, the differences are mostly around 1.5 kcal mol^{-1} (maximum 4.0 kcal mol^{-1}) for relative energies and up to 0.015 Å and 0.040 Å for C−C and C−H bond distances, respectively, but generally less (compare Tables 1 and Figures 1−4).
(21) Becke, A. D. *J. Chem. Phys.* **1993**, *98*, 5648.
(22) Lee, C.; Yang, W.; Parr, R. G. *Phys. Rev. B* **1988**, *37*, 785−789.
(23) Stephens, P. J.; Devlin, F. J.; Frisch, M. J. *J. Phys. Chem.* **1994**, *98*, 11623.
(24) Bally, T.; Sastry, G. N. *J. Phys. Chem. A* **1997**, *101*, 7923.
(25) a) Purvis, G. D.; Bartlett, R. J. *J. Chem. Phys.* **1982**, *76*, 1910. (b) Rittby, M.; Bartlett, R. J.; *J. Phys. Chem*. **1988**, *92*, 3033.
(26) Reed, A. E.; Weinhold, F. *Chem. Rev.* **1988**, *88*, 899.
(27) Hofmann, M.; Schaefer, H. F. *J. Org. Chem.* **1999**, *64*. Submitted for publication.
(28) Dinneocenzo, J. P.; Conlon, D. A. *J. Am. Chem. Soc*. **1988**, *110*, 2324.
(29) Hofmann, M.; Schaefer, H. F. Unpublished results.
(30) Williams, F.; Guo, Q.-X.; Kolb, T. M.; Nelson, S. F. *J. Chem. Soc., Commun.* **1989**, 1835.
(31) Adam, W.; Sahin, C.; Sendelbach, J.; Walter, H.; Chen, G.-F.; Williams, F. *J. Am. Chem. Soc.* **1994**, *116*, 2576.
(32) A relative energy of 17.7 kcal mol^{-1} was reported from MP3/6-31G**//6-31G* + ZPE calculations, see: Schleyer, P. v. R.; Bentley, T. W.; Koch, W.; Kos, A. J.; Schwarz, H. *J. Am. Chem. Soc.* **1987**, *109*, 6953.
(33) Jungwirth, P.; Bally, T. *J. Am. Chem. Soc.* **1993**, *115*, 5783.
(34) Ion energetics data. by Rosenstock, H. M.; Draxl, K.; Steiner, B. W.; Herron, J. T. In *NIST Chemistry WebBook, NIST Standard Reference Database Number 69*; Mallard, W. G.; Linstrom, P. J., Eds.; National Institute of Standards and Technology: Gaithersburg, MD, 1998 (http://webbook.nist.gov).
(35) Clark, T. *J. Am. Chem. Soc.* **1987**, *109*, 6838.
(36) Du, P.; Hrovat, D. A.; Borden, W. T. *J. Am. Chem. Soc.* **1988**, *110*, 3405.
(37) Nguyen, M. T.; Landuyt, L.; Vanquickenborne, L. G. *Chem. Phys. Lett.* **1991**, *182*, 225.